Dyes and Pigments 79 (2008) 176–182

Contents lists available at ScienceDirect

Dyes and Pigments

journal homepage: www.elsevier.com/locate/dyepig

A study of the binding of C.I. Direct Yellow 9 to human serum albumin using optical spectroscopy and molecular modeling

Yuanyuan Yue, Xingguo Chen *, Jin Qin, Xiaojun Yao

Department of Chemistry, Lanzhou University, Lanzhou 730000, PR China

ARTICLE INFO

Article history:
Received 2 November 2007
Received in revised form 9 February 2008
Accepted 14 February 2008
Available online 29 February 2008

Keywords:
C.I. Direct Yellow 9
Human serum albumin (HSA)
Circular dichroism (CD)
Fourier transformation infrared spectra (FT-IR)
Molecular modeling
Fluorescence

ABSTRACT

The mechanism of interaction between C.I. Direct Yellow 9 and human serum albumin was studied using spectroscopic methods including fluorescence spectra, UV–vis, Fourier transform infrared (FT-IR) and circular dichroism (CD). The quenching mechanism was investigated in terms of the association constants, number of binding sites and basic thermodynamic parameters. The distance between the human serum albumin donor and the acceptor dye was 3.64 nm as derived from fluorescence resonance energy transfer. Alteration of the secondary protein structure in the presence of the dye was confirmed by UV, FT-IR and CD spectroscopy. Molecular modeling revealed that a dye–protein complex was stabilized by hydrophobic forces and hydrogen bonding, via amino acid residues.

1. Introduction

C.I. Direct Yellow 9 (structure shown in Fig. 1) has been widely used as a dye, biological stain and diagnostic aid. Like other dyes, C.I. Direct Yellow 9 is successfully applied for clinical and medicinal purposes [1]. Some dyes were found to stain certain tissues and would destroy pathogenic organisms without causing appreciable harm to the host. As a result, some azo, thiazine and triphenyl methane dyes came into use as antiseptic trypanocides and for other medicinal purposes [2]. It was also reported that certain dyes viz., fluorescein and rose bengal were preferentially adsorbed by cancerous cells [1]. Studying structural dynamics of dye–protein complexes is crucial for understanding the biological effects and functions of dyes in body.

Human serum albumin is the major soluble protein constituents of the circulatory system, contributing significantly in the physiological functions as carrier proteins [3]. The unique feature of albumin is its ability to bind a wide variety of compounds such as metabolites, drugs, dyes, fatty acids, etc. [4], mainly because of the availability of hydrophobic pockets inside the protein network and the flexibility of the albumins to adapt its shape. The crystallographic analysis of HSA revealed that the protein, a 585-amino acid residue monomer, contains three homologous α-helical domains (I–III) and a single tryptophan (Trp214) [5]. There is evidence of conformational changes of albumin induced by its interaction with dyes and ligands. And these changes appear to affect the secondary and tertiary structure of albumin [6]. Consequently, it is important to study the interaction of dyes with serum albumin, and hence become an important research field in chemistry, life sciences and clinical medicine.

Interaction between dye and protein governs the duration and intensity of pharmacological effect [7]. Seetharamappa and coworkers have studied the binding of bromopyrogallol red and rose bengal to BSA in order to investigate that the dyes exhibit a high affinity to BSA [2,8]. Tatikolov and Costa have studied complexation of polymethine dyes with HSA [9]. In this article, we studied the binding of C.I. Direct Yellow 9 to HSA at different temperatures utilizing the fluorescence techniques in combination with UV–vis, circular dichroism (CD), Fourier transform infrared (FT-IR) spectroscopic methods. The partial binding parameters of the reaction were calculated through SGI FUEL workstations. In addition, the effect of common ions on the binding constant of C.I. Direct Yellow 9–HSA was examined.

2. Materials and methods

2.1. Materials

HSA (fatty acid-free $< 0.05\%$) and C.I. Direct Yellow 9 were used as received from Sigma Chemical Company. A molecular weight of

* Corresponding author. Tel.: +86 931 8912763; fax: +86 931 8912582.
E-mail address: chenxg@lzu.edu.cn (X. Chen).

0143-7208/$ – see front matter © 2008 Elsevier Ltd. All rights reserved.
doi:10.1016/j.dyepig.2008.02.008

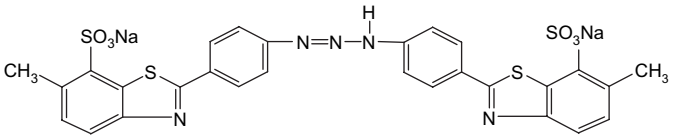

Fig. 1. The structure of C.I. Direct Yellow 9.

66,500 was taken for HSA. All other reagents were of analytical reagent grade. The double-distilled water was used throughout the experiments. NaCl (1.0 M) solution was used to maintain the ionic strength at 0.1. Tris (0.2 M)–HCl (0.1 M) buffer solution containing NaCl (0.1 M) was used to keep the pH of the solution at 7.40. Dilutions of the HSA stock (3.0×10^{-5} M) in Tris–HCl buffer solution were prepared immediately before use. The stock solution (1.0×10^{-3} M) of C.I. Direct Yellow 9 was prepared in double-distilled water.

2.2. Apparatus and methods

Fluorescence emission spectra between 310 and 550 nm were recorded on a RF-5301PC Spectrofluorimeter (Shimadzu, Japan) at 25 °C with the excitation wavelength set to 295 nm, slit widths of 5 nm for both excitation and emission bandwidths. The relative fluorescent intensity was measured in high sensitivity.

UV spectroscopy was performed on a Shimadzu UV-240 at 298 K in the range 200–500 nm using a quartz cuvette with 1 cm pathlength.

CD measurements of HSA solution alone and in the presence of C.I. Direct Yellow 9 were performed using an Olis DSM 1000 (USA) automatic recording spectrophotometer in a 1 mm cell. Each spectrum represents the average of five successive scans. CD spectra (200–300 nm) were taken at an HSA concentration of 3.0×10^{-6} M, and the results were taken as molar ellipticity ($[\theta]$) in deg cm^2 dmol^{-1}. The α-helical content of HSA was calculated from $[\theta]$ value at 208 nm using Eq. (1) [10]:

$$\alpha\text{-helix}\% = \{(-[\theta]_{208} - 4000)/(33,000 - 4000)\} \times 100 \quad (1)$$

FT-IR measurements were carried out at room temperature on a Nicolet Nexus 670 FT-IR spectrometer (America) equipped with a Germanium attenuated total reflection (ATR) accessory, a DTGS KBr detector and a KBr beam splitter. All spectra were taken via the Attenuated Total Reflection (ATR) method with resolution of 4 cm^{-1} and 60 scans. The spectra processing procedure involved collecting spectra of buffer solution under the same conditions. Next, the absorbance of the buffer solution was subtracted from the spectra of the sample solution to obtain the FT-IR spectra of the protein. The subtraction criterion was that the original spectrum of the protein solution between 2200 and 1800 cm^{-1} was featureless [11,12].

The crystal structure of HSA in complex with R-warfarin was taken from the Brookhaven Protein Data Bank (entry codes 1h9z). The potential of the 3D structure of HSA was assigned according the Amber 4.0 force field with Kollman-all-atom charges. The initial structure of all the molecules was generated by molecular modeling software Sybyl 6.9 [13]. The geometries of these compounds were subsequently optimized using the Tripos force field with Gasteiger–Marsili charges. FlexX program was applied to calculate the possible conformation of the ligands that binds to the protein. According to this kind of approach, a computational model of the target receptor was built, and partial binding parameters of the C.I. Direct Yellow 9–HSA system were calculated through SGI FUEL workstations.

For the research on the effects of metal ions, $CuCl_2$, $ZnCl_2$, $NiCl_2$, $AlCl_3$, $CrCl_3$, $HgCl_2$ and $PbCl_2$ were used as foreign substances. The anions were all chloride ions, which did not affect the protein fluorescence. The concentrations of metal ions were fixed at 3.0 μM. The fluorescence spectra of C.I. Direct Yellow 9–HSA were recorded in the presence and absence of various ions in the range 300–500 nm upon excitation at 295 nm.

3. Results and discussion

3.1. Binding properties of C.I. Direct Yellow 9 to HSA

For macromolecules, fluorescence measurements can give some information of binding small molecules to protein, such as the binding mechanism, binding mode, binding constants, binding sites and intermolecular distances. A variety of molecular interactions can result in quenching, including excited state reactions, molecular rearrangements, energy transfer, ground-state complex formation, and collisional quenching. Fig. 2 shows the fluorescence emission spectra of HSA with various amounts of C.I. Direct Yellow 9 following an excitation at 295 nm. HSA exhibited a strong fluorescence emission band at 334 nm. Its intensity decreased gradually with the addition of C.I. Direct Yellow 9. It was also observed that an increase in the fluorescence intensity at 422 nm was assigned to C.I. Direct Yellow 9. Under the same conditions, C.I. Direct Yellow 9 exhibited fluorescence emission in the range 400–500 nm which did not affect HSA intrinsic fluorescence intensity (300–375 nm). These observations may be referred to a strong binding of C.I. Direct Yellow 9 to HSA and a radiationless energy transfer between C.I. Direct Yellow 9 and HSA [14]. Moreover, the occurrence of an isobestic point at 375 nm might also indicate the existence of bound and free C.I. Direct Yellow 9 in equilibrium.

Quenching data were also used to quantitative analysis the binding of C.I. Direct Yellow 9 to HSA at different temperatures through Scatchard equation (Eq. (2)) [15]:

$$\frac{r}{D_f} = nK - rK \quad (2)$$

where r represents the number of moles of bound small molecules per mole of protein, D_f represents the molar concentration of free small molecules, n and K are the number of binding sites and binding constant, respectively. It can be seen from Fig. 3 that the Scatchard plots for the HSA–C.I. Direct Yellow 9 at different temperatures. The satisfactory linearity of Scatchard plots indicated that C.I. Direct

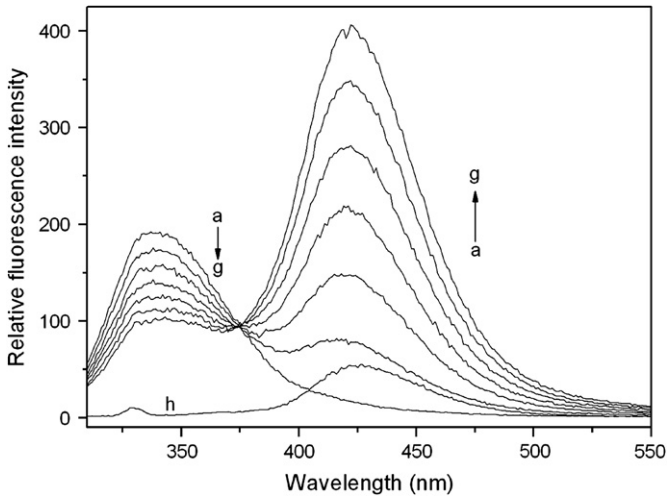

Fig. 2. The fluorescence spectra of C.I. Direct Yellow 9–HSA system. The concentration of C.I. Direct Yellow 9 corresponding to 0, 1.66, 3.32, 4.98, 6.62, 8.26, 9.90 μM from (a) to (g); [HSA] = 3.0 μM; (h) 1.66 μM C.I. Direct Yellow 9; λ_{ex} = 295 nm, λ_{em} = 334 nm; pH = 7.40; T = 298 K.

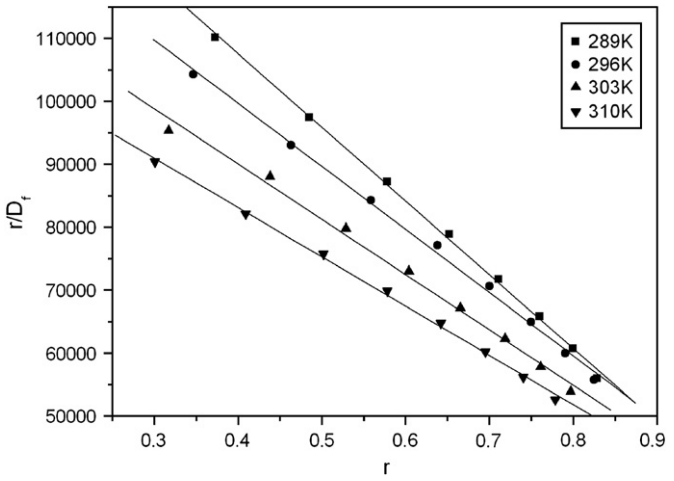

Fig. 3. The Scatchard plot for the HSA–C.I. Direct Yellow 9 system at different temperatures. [HSA] = 3.0 μM; [C.I. Direct Yellow 9] = 3.32–14.78 μM; pH = 7.40; λ_{ex} = 295 nm and λ_{em} = 334 nm.

Yellow 9 bound to a class of binding sites on HSA with the increase of the temperature. The binding constants at four temperatures are shown in Table 1 and are used to calculate the thermodynamics parameters. Since higher temperatures result in larger diffusion coefficients, the quenching constants are expected to increase with temperature. In contrast, elevated temperature decreases the stability of complexes and thus lowers the values of the static quenching constants. Table 1 indicates that the quenching mechanism of fluorescence of HSA by C.I. Direct Yellow 9 was most likely a static quenching procedure.

3.2. Binding mode

Essentially, there are four types of non-covalent interaction existing in ligand binding to proteins. These are hydrogen bond, van der Waals force, electrostatic force, hydrophobic interaction force. The signs and magnitudes of thermodynamic parameters for protein reactions can account for the main forces contributing to protein stability. If the enthalpy changes (ΔH^0) do not vary significantly over the temperature range studied, then its value can be determined from the Van't Hoff equation (Eq. (3)) [16]:

$$\ln K = -\Delta H^0/RT + \Delta S^0/R \quad (3)$$

where K is the binding constant at a definite temperature and R the gas constant. A linear plot of ln K against $1/T$ yields ΔH^0 and ΔS^0 for the binding interaction. Consequently, the amount of free energy change required for the binding is estimated from Eq. (4):

$$\Delta G^0 = \Delta H^0 - T\Delta S^0 \quad (4)$$

From the linear relationship between ln K and the reciprocal absolute temperature, the value of ΔH^0 and ΔS^0 can be obtained. The results of ΔG^0 at different temperatures, calculated using Eq. (4), are presented in Table 1. As shown in Table 1, the signs for ΔH^0 and ΔS^0 of the binding reaction between C.I. Direct Yellow 9 and HSA were found to be negative and positive, respectively. Thus, the formation of the complex was an exothermic reaction accompanied by positive ΔS^0 value. Ross and Subramanian [17] have characterized the sign and magnitude of the thermodynamic parameter associated with various individual kinds of interaction that may take place in protein association processes, as described below. From the point of view of water structure, a positive ΔS^0 value is frequently taken as a typical evidence for hydrophobic interaction. Furthermore, the negative ΔH^0 value (−14.27 kJ mol^{-1}) observed cannot be mainly attributed to electrostatic interactions since for electrostatic interactions ΔH^0 is very small, almost zero [17,18]. Negative ΔH^0 value is observed whenever there is hydrogen bonding in the binding [18]. The negative ΔH^0 and positive ΔS^0 values for the interactions between C.I. Direct Yellow 9 and HSA indicated that both hydrophobic and hydrogen bond interactions played a role in the binding reaction.

Table 1
Binding parameters and thermodynamic parameters of C.I. Direct Yellow 9–HAS

pH	T (K)	K ($\times 10^5$ M^{-1})	R^a	n	ΔG^0 (kJ mol^{-1})	ΔS^0 (J mol^{-1} K^{-1})	ΔH^0 (kJ mol^{-1})
7.4	289	1.17	0.9992	1.01	−28.03	47.62	−14.27
	296	1.01	0.9985	1.04	−28.37		
	303	0.88	0.9967	1.06	−28.70		
	310	0.78	0.9991	1.09	−29.03		

[a] The correlation coefficient.

3.3. Effect of C.I. Direct Yellow 9 on the HSA conformation

3.3.1. Synchronous fluorescence studies

Synchronous fluorescence spectroscopy introduced by Llody [19] has been used to characterize complex mixtures providing fingerprints of complex samples [20]. In the synchronous spectra, the sensitivity associated with fluorescence is maintained while offering several advantages: spectral simplification, spectral bandwidth reduction and avoiding different perturbing effects. It is well known that the fluorescence of HSA comes from the tyrosine, tryptophan, and phenylalanine residues. According to the theory of Miller [21], when $\Delta\lambda = 60$ nm, the spectrum characteristic of the protein tryptophan residues was observed [22]. A faint blue shift (from 341 to 338 nm) can be observed from the synchronous fluorescence spectra of interaction between C.I. Direct Yellow 9 and HSA. The faint blue-shift effect expresses the change in conformation of HSA. It is also indicated that the polarity around the tryptophan residues was decreased and the hydrophobicity was increased.

3.3.2. UV, CD, FT-IR spectral studies

UV–vis absorption measurement is a very simple method and applicable to explore the structural change [23] and know the complex formation. In the present study, we measured the UV–vis absorbance spectra of HSA with various amounts of C.I. Direct Yellow 9. Fig. 4 shows the UV–vis absorption spectra of HSA from 200 to 500 nm in Tris buffer solution in the presence of different C.I. Direct Yellow 9 concentrations. C.I. Direct Yellow 9 was almost non-UV absorption under the presence experiment conditions. As can be seen from Fig. 4, HSA has strong absorbance with a peak at 210 nm and the absorbance of HSA increased with the addition of C.I. Direct Yellow 9; the chromophore of HSA–C.I. Direct Yellow 9 gives a very specific pattern of the UV–vis spectrum with a slight triple absorbance spectra at higher concentration of C.I. Direct Yellow 9 in the system, and the addition of C.I. Direct Yellow 9 results in the evident shift of C.I. Direct Yellow 9–HSA spectrum towards longer wavelength (from 212 to 216 nm). A reasonable explanation for the two evidences may come from the interaction between C.I. Direct Yellow 9 and HSA [24]. It also suggested that small structural change of HSA upon interaction with C.I. Direct Yellow 9.

Further evidence of conformational changes of HSA upon addition of C.I. Direct Yellow 9 was provided by CD data. CD is a sensitive technique to monitor conformational changes in protein upon interaction with ligand. CD spectra of HSA with various concentrations of C.I. Direct Yellow 9 are shown in Fig. 5. It was apparently observed that CD spectral bands of HSA were at 208 and 222 nm, characteristic of α-helical structure of protein. The reasonable

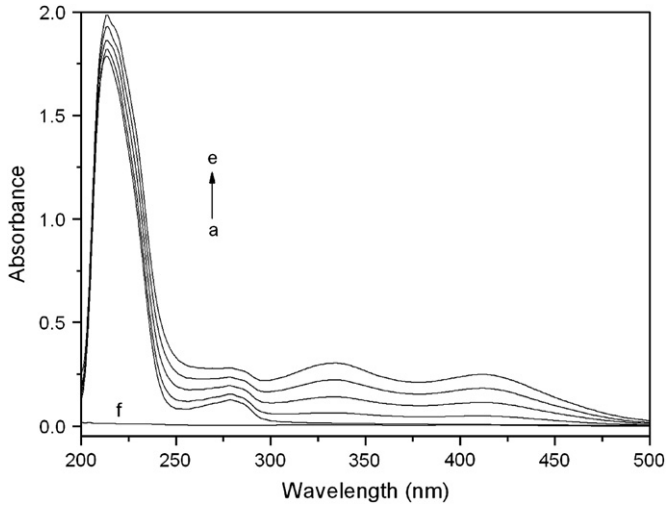

Fig. 4. UV absorption spectra of HSA. HSA concentration was at 3 μM (a) and C.I. Direct Yellow 9 concentration for HSA–C.I. Direct Yellow 9 system was at 1.66, 3.32, 4.98, 6.62, 8.26 μM (b–e). A concentration of 1.66 μM C.I. Direct Yellow 9 (f) was used for C.I. Direct Yellow 9 only. pH = 7.40, $T = 298$ K.

explanation is that both the negative peaks between 208–209 and 222–223 nm are contributed to $n \rightarrow \pi^*$ transfer for the peptide bond of α-helical [25]. As shown in Fig. 5, the binding of C.I. Direct Yellow 9 to HSA caused only a decrease in negative ellipticity without significant shift of the peaks, indicating that C.I. Direct Yellow 9 induced a slight decrease in the α-helix structure content of the protein. However, the CD spectra of HSA in the presence and absence of C.I. Direct Yellow 9 were similar in shape, indicating that the structure of HSA was also predominantly α-helix. From the above results, it was apparent that the effect of C.I. Direct Yellow 9 on HSA caused a conformational change of the protein, with the loss of helical stability. The α-helical content of HSA was calculated from Eq. (1). The calculated results exhibited a reduction of α-helical structures from 54.11 to 52.88 and 51.99% at a molar ratio of HSA to C.I. Direct Yellow 9 of 1:1, 1:2, respectively.

FT-IR spectroscopy has been proven to be a powerful tool for providing conformational and structural dynamics information of proteins. Infrared spectra of proteins exhibit a number of the amide bands, which represent different vibrations of the peptide moiety. Among the amide bands of the protein, amide I band ranging from 1600 to 1700 cm^{-1} (mainly C═O stretch) and amide II band ≈1548 cm^{-1} (C–N stretch coupled with N–H bending mode) have been widely accepted as the typical ones to be used [25]. They both have a relationship with the secondary structure of the protein. However, the amide I band is more sensitive to the change of protein secondary structure than amide II [26]. Fig. 6 shows the FT-IR spectra of the free HSA and its C.I. Direct Yellow 9 complexes in Tris–HCl buffer solution at 298 K. As shown in Fig. 6, the peak position of amide I band (1639.22 cm^{-1}), amide II band (1554.37 cm^{-1}) shifted after addition of C.I. Direct Yellow 9 and the intensities of the amide I increased in the spectra of free HSA. These results indicated that C.I. Direct Yellow 9 interacted with the C═O and C–N groups in the protein polypeptides. The C.I. Direct Yellow 9–protein complexes caused the rearrangement of the polypeptide carbonyl hydrogen bonding network and finally the reduction of the protein α-helical structure.

3.4. The energy transfer between C.I. Direct Yellow 9 and HSA

Fluorescence resonance energy transfer (FRET) is a distance-dependent interaction between the different electronic excited states of dye molecules in which excitation energy is transferred from one molecular (donor) to another molecular (acceptor) system without emission of a photon from the former molecular system. According to the Förster non-radiative resonance energy transfer theory [27], the rate of energy transfer depends on the following conditions: (a) the donor can produce fluorescent light that has sufficiently long lifetime; (b) the fluorescence emission spectrum of the donor and the UV absorbance spectrum of the acceptor have more overlap; (c) the distance between the donor and the acceptor is small (1–10 nm) [28]. Here the donor and acceptor are HSA and C.I. Direct Yellow 9, respectively. The absorption spectrum of C.I. Direct Yellow 9 (1.0×10^{-6} M) was recorded in the range of 300–500 nm in the pH 7.40 Tris buffer. The emission spectrum of HSA (1.0×10^{-6} M) was also recorded under the same condition. There was a spectral overlap between the fluorescence emission spectrum of HSA and UV–vis absorption spectrum of C.I. Direct Yellow 9 (Fig. 7). As the fluorescence emission of protein was affected by the excitation light around 295 nm, the spectrum ranging from 300 to 500 nm was chosen to calculate the overlapping integral. The efficiency (E) of energy transfer from donor to acceptor is

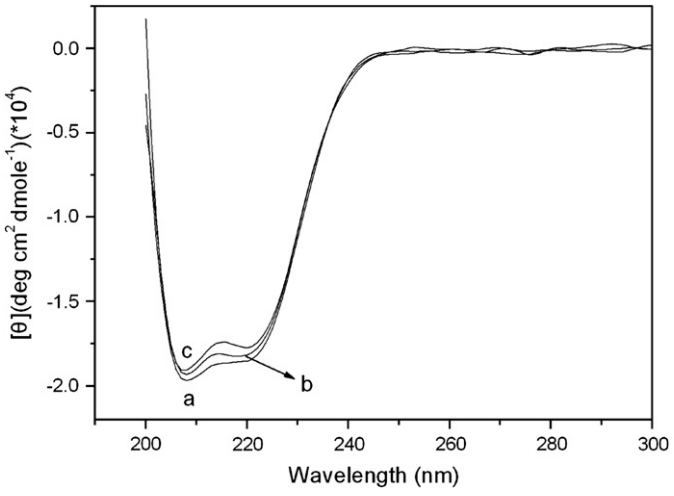

Fig. 5. CD spectra of the HSA–C.I. Direct Yellow 9 system. (a) 3.0 μM HSA; (b) 3.0 μM HSA + 3.0 μM C.I. Direct Yellow 9; (c) 3.0 μM HSA + 6.0 μM C.I. Direct Yellow 9; pH = 7.40, $T = 298$ K.

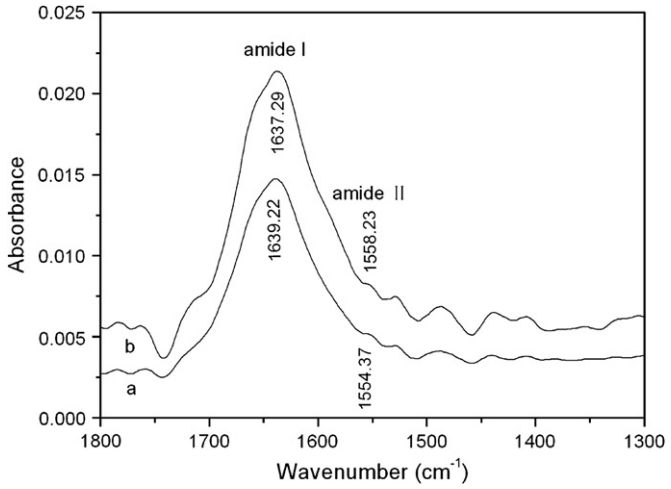

Fig. 6. FT-IR spectra of free HSA (a) and difference spectra [(HSA solution + C.I. Direct Yellow 9 solution)–(C.I. Direct Yellow 9 solution)] (b) in buffer solution in the region of 1800–1300 cm^{-1}, [HSA] = 3.0×10^{-5} M, [C.I. Direct Yellow 9] = 6.0×10^{-5} M, pH = 7.40, $T = 298$ K.

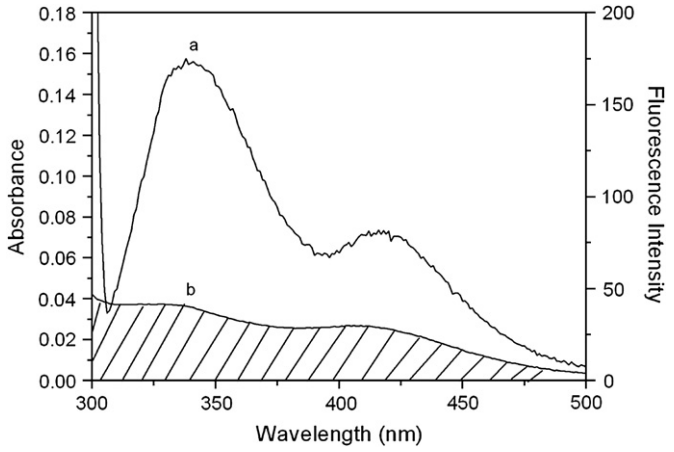

Fig. 7. Overlapping between the fluorescence emission spectrum of HSA (a) and absorption UV spectrum of C.I. Direct Yellow 9 (b). $C_{\text{C.I. Direct Yellow 9}} = C_{\text{HSA}} = 1.0 \times 10^{-6}$ M. pH = 7.40, $T = 298$ K.

related to the distance (R) in this case between HSA and C.I. Direct Yellow 9 according to Eq. (5):

$$E = 1 - F/F_0 = R_0^6/\left(R_0^6 + r^6\right) \tag{5}$$

where F_0 and F are the fluorescence intensities without and with C.I. Direct Yellow 9, respectively, r is the binding distance between donor and receptor, and R_0 is the Förster critical distance between donor and acceptor, at which 50% of the excitation energy is transferred to acceptor and can be obtained from donor emission and acceptor absorption spectra using Eq. (6):

$$R_0^6 = 8.79 \times 10^{-25} K^2 N^{-4} \Phi J \tag{6}$$

In Eq. (6), K^2 is the orientation factor related to the geometry of the donor and acceptor of dipoles; N is the average refractive index of medium in the wavelength range where spectral overlap is significant. Φ is the fluorescence quantum yield of the donor from Trp in HSA, and J is the overlap integral of the fluorescence emission spectrum of the donor and the absorption spectrum of the receptor. Therefore,

$$J = \left(\sum F(\lambda)\varepsilon(\lambda)\lambda^4 \Delta\lambda\right) \Big/ \left(\sum F(\lambda)\Delta\lambda\right) \tag{7}$$

where $F(\lambda)$ is the fluorescence intensity of the fluorescence donor when the wavelength is λ, $\varepsilon(\lambda)$ is the molar absorptivity of the receptor at wavelength of λ. On the basis of these relationships, J, E and R_0 can be calculated; then, the value of r also can be calculated.

The orientation factor (K^2) is commonly taken as 2/3, assuming a random orientation for both the donor and the acceptor. This value is reasonable for the present system, as the tryptophan chromophore rotates very fast in the protein. The refractive index (N) of water is 1.336, $\Phi = 0.118$ [29], according to Eqs. (5)–(7), we could calculate that $R_0 = 3.26$ nm; $E = 0.34$ and $r = 3.64$ nm. Obviously, the acceptor–donor distance is less than 8 nm [30], which implied that the energy transfer is from HSA to C.I. Direct Yellow 9 occurred with high possibility. Further the value of r obtained this way agrees very well with literature value of substrate binding to serum albumin at site II A [14].

3.5. Molecular modeling

Crystal structure analysis has revealed that HSA consists of a single polypeptide chain of 585-amino acid residues and comprises three structurally homologous domains (I–III): I (residues 1–195), II (196–383), III (384–585), that assemble to form a heart-shaped molecule, and each domain includes two subdomains called A and B to form a cylinder and each subdomain involves 6 and 4 α-helixes, respectively, the only Trp residue (Trp214) located in subdomain IIA. Almost all hydrophobic amide acids are embedded in the cylinders forming hydrophobic cavities, which play an important role on absorption, metabolism, and transportation of

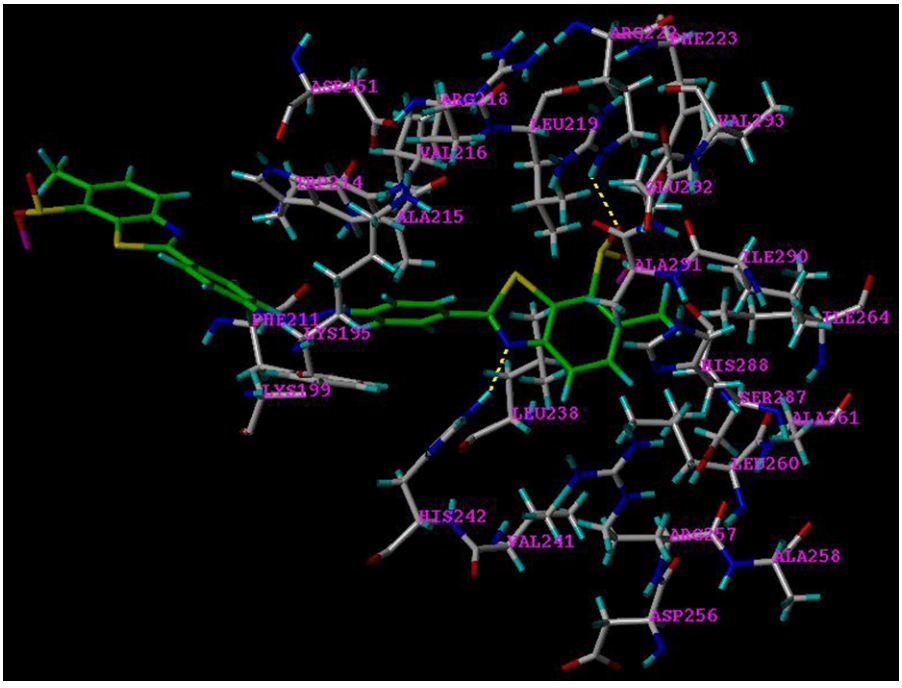

Fig. 8. The interaction model between C.I. Direct Yellow 9 and HSA. Only residues around 6.5 Å of the ligand are displayed. The residues of HSA are represented using gray ball and stick model and the C.I. Direct Yellow 9 structure is represented by a green one. The hydrogen bond between C.I. Direct Yellow 9 and HSA is represented by yellow dashed line. (For interpretation of the references to color in this figure legend, the reader is referred to the web version of this article.)

Table 2
Effects of some common ions and toxic ions (3.0 μM) on HSA–C.I. Direct Yellow 9 system

System	Binding constant ($\times 10^5$ M^{-1})	R^a
HSA + C.I. Direct Yellow 9	0.98	0.9987
HSA + C.I. Direct Yellow 9 + Zn^{2+}	0.89	0.9980
HSA + C.I. Direct Yellow 9 + Ni^{2+}	0.97	0.9997
HSA + C.I. Direct Yellow 9 + Al^{3+}	0.91	0.9967
HSA + C.I. Direct Yellow 9 + Cu^{2+}	0.84	0.9994
HSA + C.I. Direct Yellow 9 + Cr^{3+}	0.95	0.9936
HSA + C.I. Direct Yellow 9 + Hg^{2+}	0.87	0.9987
HSA + C.I. Direct Yellow 9 + Pb^{2+}	0.86	0.9991

[a] The correlation coefficient.

biomolecule. Some studies have proved that HSA is able to bind many ligands in several binding sites [31]. The best energy ranked results of the binding mode between C.I. Direct Yellow 9 and HSA is shown in Fig. 8 (only residues around 6.5 Å of C.I. Direct Yellow 9 was displayed). The docking showed that C.I. Direct Yellow 9 was located within the binding pocket of subdomain IIA of the protein (The Warfarin Binding Pocket), and C.I. Direct Yellow 9 were adjacent to hydrophobic residues Leu238, Trp214 of subdomain IIA of HSA. Furthermore, this phenomenon provided a good structural basis to explain the very efficient fluorescence quenching of HSA emission in the presence of C.I. Direct Yellow 9. On the other hand, there was hydrogen interaction between $-SO_3$ of C.I. Direct Yellow 9 and the residues Leu219. The results indicated that the formation of hydrogen bond decreased the hydrophilicity and increased the hydrophobicity to make the C.I. Direct Yellow 9–HSA system stable. The calculated binding Gibbs free energy (ΔG^0) was −22.86 kJ/mol, which was not very close to the experimental data (−28.03 kJ/mol) to some degree. A possible explanation may be that the X-ray structure of the protein from crystals differs from that of the aqueous system used in this study. Therefore, the results obtained from modeling indicated that the interaction between C.I. Direct Yellow 9 and HSA was dominated by hydrophobic force, and also the existence of hydrogen bonds.

3.6. The effect of common ions and toxic ions on the binding constant

In plasma, there are some metal ions, especially the bivalent type, which are essential in the human body. Some references reported that Cu^{2+}, Zn^{2+}, Ni^{2+}, Al^{3+}, Cr^{3+} and other metal ions can form complexes with serum albumins. The effect of common ions on the binding constants was investigated at 298 K by recording the fluorescence intensity in the range of 300–500 nm upon excitation at 295 nm. The results are summarized in Table 2. In addition, we have also investigated the influence of toxic ions viz., Hg^{2+} and Pb^{2+} on the binding of C.I. Direct Yellow 9 to HSA. The presence of inhibitors reduced the C.I. Direct Yellow 9–HSA binding constants. This is likely caused by a conformational change in the vicinity of the binding site. However, the formation of metal ion–HSA complexes is likely to effect changes in the conformation of the protein, which may affect C.I. Direct Yellow 9 binding kinetics and could even inhibit C.I. Direct Yellow 9–HSA interaction. The binding constant decreased implying that inhibitors may enhance the toxic effects and decrease the activity of HSA.

4. Conclusions

The interaction of C.I. Direct Yellow 9 with HSA under simulated physiological condition (pH 7.4, ionic strength 0.1) was studied by different optical techniques and molecular modeling. The results indicated that the probable mechanism of C.I. Direct Yellow 9 interaction with HSA is a static quenching process. The binding process was exothermic and spontaneous, as indicated by the thermodynamic parameters analyzed. The molecular docking study and thermodynamic analysis suggested that C.I. Direct Yellow 9 could bind HSA through the hydrophobic force, hydrogen bond between C.I. Direct Yellow 9 and HSA residue. On the efficiency of energy transfer between the donor and acceptor, the distance between the fluorophore (Trp214) of HSA and the dye of C.I. Direct Yellow 9 was estimated to be $r = 3.64$ nm. Fluorescence, UV–vis and CD spectra showed that the C.I. Direct Yellow 9 adsorbed to HSA under the studied conditions induced small changes in the structure of HSA.

Acknowledgements

We are grateful for financial support from the National Natural Science Foundation of China (No. 20275014).

References

[1] Kamat BP, Seetharamappa J. Fluorescence and circular dichroism studies on the interaction of bromocresol purple with bovine serum albumin. Polish Journal of Chemistry 2004;78:723–32.
[2] Shaikh SMT, Seetharamappa J, Ashoka S, Kandagal PB. A study of the interaction between bromopyrogallol red and bovine serum albumin by spectroscopic methods. Dyes and Pigments 2007;73:211–6.
[3] Peters TJ. All about albumin. London: Academic Press; 1996.
[4] Waheed AA, Sridhar Rao K, Gupta PD. Mechanism of dye binding in the protein assay using eosin dyes. Analytical Biochemistry 2000;287:73–9.
[5] He JX, Carter DC. Atomic structure and chemistry of human serum albumin. Nature 1992;358:209–15.
[6] Hushcha TO, Luik AL, Naboka YN. Conformation changes of albumin in its interaction with physiologically active compounds as studied by quasi-elastic light scattering spectroscopy and ultrasonic method. Talanta 2000;53:29–34.
[7] Eftink MR, Ghiron CA. Fluorescence quenching of indole and model micelle systems. Journal of Physical Chemistry 1976;80:486–93.
[8] Shaikh SMT, Seetharamappa J, Kandagal PB, Manjunatha DH, Ashoka S. Spectroscopic investigations on the mechanism of interaction of bioactive dye with bovine serum albumin. Dyes and Pigments 2007;74:665–71.
[9] Tatikolov AS, Costa SMB. Complexation of polymethine dyes with human serum albumin: a spectroscopic study. Biophysical Chemistry 2004;107:33–49.
[10] Khan AM, Muzammil S, Musarrat J. Differential binding of tetracyclines with serum albumin and induced structural alterations in drug-bound protein. International Journal of Biological Macromolecules 2002;30:243–9.
[11] Dong A, Huang P, Caughey WS. Protein secondary structures in water from second-derivative amide I infrared spectra. Biochemistry 1990;29:3303–8.
[12] Liu JQ, Tian JM, Tian X, Hu ZD, Chen XG. Interaction of isofraxidin with human serum albumin. Bioorganic and Medicinal Chemistry 2004;12:469–74.
[13] Morris G. SYBYL software, version 6.9. St. Louis: Tripos Associates Inc.; 2002.
[14] Deepa S, Mishra AK. Fluorescence spectroscopic study of serum albumin–bromadiolone interaction: fluorimetric determination of bromadiolone. Journal of Pharmaceutical and Biomedical Analysis 2005;38:556–63.
[15] Scatchard G. The attractions of protein for small molecules and ions. Annals of the New York Academy of Sciences 1949;51:660–73.
[16] Bi SY, Song DQ, Tian Y, Zhou X, Liu ZY, Zhang HQ. Molecular spectroscopic study on the interaction of tetracyclines with serum albumins. Spectrochimica Acta Part A Molecular and Biomolecular Spectroscopy 2005;61:629–36.
[17] Ross PD, Subramanian S. Thermodynamics of protein association reactions: forces contributing to stability. Biochemistry 1981;20:3096–102.
[18] Rahman MH, Maruyama T, Okada T, Yamasaki K, Otagiri M. Study of interaction of carprofen and its enantiomers with human serum albumin-I: mechanism of binding studied by dialysis and spectroscopic methods. Biochemical Pharmacology 1993;46:1721–31.
[19] Llody JBF. Synchronized excitation of fluorescence emission spectra. Nature Physical Science 1971;231:64–5.
[20] Apicella B, Ciajolo A, Tregrossi A. Fluorescence spectroscopy of complex aromatic mixtures. Analytical Chemistry 2004;76:2138–43.
[21] Miller JN. Recent advances in molecular luminescence analysis. Proceedings of the Analytical Division of the Chemical Society 1979;16:203–8.
[22] Wang YP, Wei YL, Dong C. Study on the interaction of 3,3-bis (4-hydroxy-1-naphthyl)-phthalide with bovine serum albumin by fluorescence spectroscopy. Journal of Photochemistry and Photobiology A Chemistry 2006;177:6–11.
[23] Hu YJ, Liu Y, Wang J, Xiao X, Qu SS. Study of the interaction between monoammonium glycyrrhizinate and bovine serum albumin. Journal of Pharmaceutical and Biomedical Analysis 2004;36:915–9.
[24] He WY, Li Y, Xue CX, Hu ZD, Chen XG, Sheng FL. Effect of Chinese medicine alpinetin on the structure of human serum albumin. Bioorganic and Medicinal Chemistry 2005;13:1837–45.
[25] Yang P, Gao F. The principle of bioinorganic chemistry. Science Press; 2002. p. 349.

[26] Witold KS, Henry HM, Dennis C. Determination of protein secondary structure by Fourier transform infrared spectroscopy: a critical assessment. Biochemistry 1993;32:389–94.
[27] Sklar LA, Hudson BS, Simoni RD. Conjugated polyene fatty acids as fluorescent probes: binding to bovine serum albumin. Biochemistry 1977;16:5100–8.
[28] Forster T. In: Sinanoglu O, editor. Modern quantum chemistry, vol. 3. New York: Academic Press; 1996. p. 93.
[29] Epps DE, Raub TJ, Caiolfa V, Chiari A, Zamai M. Evaluating the binding selectivity of transthyretin amyloid fibril inhibitors in blood plasma. The Journal of Pharmacy and Pharmacology 1998;51:41–8.
[30] Valeur B, Brochon JC. New trends in fluorescence spectroscopy. 6th ed. Berlin: Springer Press; 1999. p. 25.
[31] Kragh-Hansen U. Molecular aspect of ligand binding to serum albumin. Pharmacological Review 1981;33:17–53.